ISSN 2522-9117 (print), ISSN 2786-6149 (online)
"Фундаментальні та прикладні проблеми чорної металургії". 2025. Випуск 39
"Fundamental and applied problems of ferrous metallurgy". 2025. Issue 39

https://doi.org/10.52150/2522-9117-2025-39-19

УДК 621.376.9:535.551.047:546.241

I. M. Liubeka[1,*], Head of Production Department, ORCID 0009-0005-2440-5496
K. V. Agarkov[1], Crystal Growth Operator, ORCID 0000-0002-3418-3664

[1]*LLC "Crys-Teh", Ukraine*

[*] *Corresponding author: i.liubeka@crys-teh.com*

ACOUSTO-OPTIC DEVICES BASED ON TeO_2 CRYSTALS: SPACE SPECTROMETRY, MEDICINE, AND QUANTUM SYSTEMS. (REVIEW)

Abstract. Tellurium dioxide (TeO_2, paratellurite) remains a key material in photonics thanks to its high acousto-optic figure of merit, birefringence, and wide transparency. Devices based on TeO_2 - modulators, deflectors, and tunable filters - are widely used for beam control, spectral selection, and polarization. This review article examines in detail three major domains where TeO_2-based devices have become critical: space spectrometry, medicine, and quantum technologies. In space exploration, acousto-optic tunable filters (AOTFs) fabricated from TeO_2 are implemented in flagship instruments such as ESA's NOMAD on ExoMars, NASA's SuperCam on the Perseverance rover, and China's Chang'e spectrometers. These instruments enable high-resolution, in spectral analyses of planetary surfaces and atmospheres, providing insights into mineralogy, volatiles, and habitability. In the medical domain, Acousto-optic frequency shifters (AOFS) and fiber-based laser Doppler vibrometers exploit TeO_2 to achieve precise, non-invasive measurements of middle ear ossicle vibrations, offering clinicians a novel diagnostic tool in otology. These systems, benefiting from the safety and versatility of telecom-band radiation, illustrate how AO devices can address unmet clinical needs. The translation of TeO_2-based devices into medicine highlights the interdisciplinary role of acousto-optics, bridging physics, engineering, and healthcare.Quantum technologies represent perhaps the most transformative frontier. Here, TeO_2-based acousto-optic modulators and deflectors are indispensable for photon-level control: fast frequency shifting, phase stabilization, routing, and generation of spatial modes of light. Their ability to integrate into bi-frequency interferometers and multi-channel quantum networks places them at the foundation of the emerging quantum internet, quantum communication protocols, and scalable quantum computing. Overall, such promising application areas require not only scaling up crystal production but also continuous improvement of their quality. The purpose of this review is to demonstrate concrete examples of how TeO_2 devices are applied across such diverse fields, underlining their continued importance for next-generation photonics.

Keywords: tellurium dioxide, acousto-optic devices, acousto-optic tunable filter, acousto-optic modulator, acousto-optic frequency shifters, space spectrometry, quantum communication, quantum interferometry.

For citation: Liubeka, I. M., & Agarkov, K. V. (2025). Acousto-optic devices based on TeO_2 crystals: space spectrometry, medicine, and quantum systems. (Review). *Fundamental and applied problems of ferrous metallurgy*, 39, 309-324. https://doi.org/10.52150/2522-9117-2025-39-19

Introduction

Single crystals of tellurium dioxide (TeO_2, paratellurite) have remained a mainstay of applied photonics for more than half a century [1]. The combination of high birefringence, a strong photoelastic response, and low acoustic velocities yields one of the best acousto-optic figures of merit [1]. As a result, large diffraction efficiencies and wide optical apertures can be achieved with modest RF power - critical for modern laser systems without compromises in stability, footprint, or power consumption.

Today, devices based on TeO_2 single crystals underpin an ecosystem of components: acousto-optic modulators (AOMs) [2] and deflectors (AODs) [2] for controlling beam intensity, frequency, and direction; acousto-optic tunable filters (AOTFs) [3] for non-mechanical spectral selection; and polarization prisms and polarizers exploiting natural birefringence. These elements are integrated into solid-state and fiber lasers (Q-switching, pulse picking, frequency shifting) [4], beam-positioning and scanning systems, and advanced spectral-imaging platforms - from hyperspectral cameras to spectroscopic modules used in materials science, biomedical diagnostics, and cultural-heritage studies [5].

Applications in spectral imaging are progressing particularly rapidly. AOTF cameras provide continuous, rapid wavelength tuning with no moving parts, enabling acquisition of data cubes with high repeatability and compact optics. In active-imaging lidar, this capability enables simultaneous ranging and spectral discrimination of targets; in art conservation, it supports mapping of pigments and degradation products; and in chemical and biomedical diagnostics, it enables fast, selective analyses without sample preparation. In optoelectronics and quantum technologies, TeO_2-based AOMs/AODs remain standards for frequency shifting, phase stabilization, and beam routing down to the single-photon regime [2, 6].

Space spectrometry

The acousto-optic tunable filter (AOTF) is an electronically tunable dispersive optical device without any moving parts. It can change the wavelength of the output diffracted light by controlling the input radio frequency (RF) [7]. Harris and Wallace first proposed a collinear AOTF in

1969 [8]. In 1974, Chang et al. used TeO_2 to construct a noncollinear AOTF [9], which overcame the drawbacks of the collinear AOTF in terms of limited crystal availability and complicated design. In 1987, an AOTF spectrometer was used for ocean observations in the Soviet satellite "Ocean-O1-N2" [10]. In 2003, the SPICAM instrument onboard the European Space Agency's Mars Express mission realized the first deep space application of AOTF for Martian atmospheric analysis (SPICAM IR Spectrometer) [11].

Recent decades AOTF-based spectrometers have been successfully integrated into flagship projects such as the Chinese Chang'e lunar program (VNIS and LMS instruments), ESA's ExoMars Trace Gas Orbiter (NOMAD spectrometer), and NASA's Mars 2020 Perseverance (SuperCam) [12, 13, 14]. These instruments have demonstrated the ability of AOTFs to perform in situ spectral measurements directly on extraterrestrial surfaces, enabling mineralogical mapping, water and hydroxyl detection, and atmospheric gas analysis with high spectral resolution and robustness.

The SuperCam infrared spectrometer operates by scanning the entire spectral range with an Acousto-Optic Tunable Filter (AOTF), building on the successful heritage of the AOTF used in the SPICAM instrument [14, 15]. The AOTF functions by diffracting incident light through traveling acoustic waves generated in a birefringent tellurium dioxide (TeO_2) crystal by an electro-acoustic transducer. According to Bragg diffraction theory, the acoustic wavefront acts like a dynamic thick grating: when the phase-matching condition is satisfied, a single monochromatic diffracted beam emerges, deviated from the main undiffracted polychromatic beam. The central wavelength of the diffracted beam is directly determined by the acoustic wave frequency (set by the RF driving signal), while the spectral bandwidth depends on the geometry of the crystal [16].

Because TeO_2 is birefringent, the interaction generates two symmetric pairs of beams: an ordinary (o-ray) and an extraordinary (e-ray), each producing diffracted and undiffracted outputs (fig. 1).

These pairs have identical spectral properties but are orthogonally polarized. In the SuperCam spectrometer, the undiffracted zero-order beam is suppressed in a light trap, while the e-ray and o-ray beams are separated and directed to two individual photodiodes via dedicated ZnSe optics (fig. 2).

The optical train of the instrument consists of:

- an entrance aperture illuminated by the MU telescope, defining the spectrometer's field of view,
- a folding mirror and a ZnSe collimator lens,
- the AOTF crystal itself,
- a ZnSe objective lens that focuses the three AOTF outputs (with the zero-order trapped, and the e- and o-rays transmitted),

- two photodiodes, each with a ZnSe relay lens imaging the entrance aperture onto the detector. The e-ray beam path is folded before reaching its photodiode.

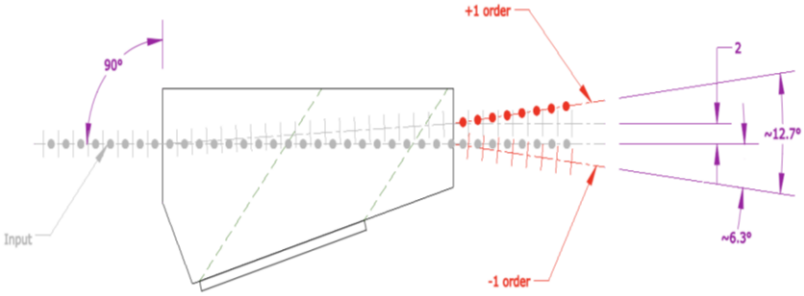

Figure 1. Schematic diagram presenting the AOTF diffraction principle. The +1-order stands for the o-order, while the -1-order stands for the e-order. The beam labelled 2 represents the undiffracted beam. ©Gooch & Housego [16].

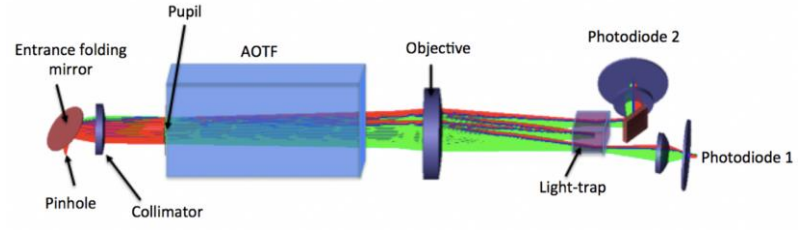

Figure 2. Optical design of the SuperCam infrared spectrometer [16].

The AOTF is the core component of the spectrometer and was designed and built by Gooch & Housego (Ilminster, UK). It weighs 84 g and was engineered to stabilize the two polarized diffracted outputs at ±3 mrad across the full RF frequency range. The angular separation between the diffracted orders and the zero-order is greater than 6°, while the zero-order beam is kept within 0.5° of the input direction to allow efficient trapping and minimize stray light inside the IRBOX. The device supports a maximum acceptance angle of 4° for the incoming beam. Extensive qualification tests confirmed that these specifications are met under representative operational conditions.

The SPICAM IR Spectrometer was equipped with a TeO_2 AOTF aperture of 3.6 × 3.6 mm², ±3.5° [11]. In contrast, the later NOMAD spectrometer featured two channels with apertures of 5 mm and 15 mm ±3° and ±2.15° respectively [14].

Next-generation spectrometers were being designed as part of NASA Ames's contribution to Artemis - specifically under the Near Infrared Volatiles Spectrometer System (NIRVSS), aimed at detecting volatiles in the near-IR and mapping water-bearing minerals on the Moon.

However, in 2025 the manufacturer reported that the NASA spaceflight program for which Brimrose had been named a contractor was canceled. By then, the company had already built four customized AOTF spectrometers; all had passed rigorous testing and were space-qualified to search for hydroxyl crystals on the lunar surface. The first of these instruments was launched into space, but due to rocket technical problems it never reached the Moon [17].

Meanwhile, China has been rapidly expanding its own line of AOTF spectrometers within the Chang'e program, advancing capabilities for remote sensing of volatiles and minerals.

The Chinese Chang'e Project has implemented three AOTF spectrometers for in situ spectral measurement of the lunar surface: the visible and near-infrared imaging spectrometers (VNIS) onboard Chang'e-3 (2013) [18] and Chang'e-4 (2018) [19] unmanned lunar rovers and the lunar mineralogical spectrometer (LMS) onboard Chang'E-5 (2020) [20]. VNIS onboard Chang'e-3 was the first instrument to realize in situ imaging spectral measurement of the lunar surface. The main objectives of the mission are to perform visible and near-infrared spectral imaging (400-900 nm) and short-wave infrared spectral measurements (900-2400 nm) of the lunar surface targets. The VNIS can obtain spectral and geometric imaging data of objects on the lunar surface. The mission also focused on accomplishing in situ analyses of the mineral composition, content (abundance), and chemical composition of probe sites in the patrol area. A specific performance comparison of the instruments is listed in table 1.

Table 1. Main performance parameters of VNIS and LMS [12].

Parameters	VNIS/Chang'e-3		VNIS/Chang'e-4		LMS/Chang'e-5	
	VIS-NIR	SWIR	VIS-NIR	SWIR	VIS-NIR	IR
Spectral coverage/nm	449–950	900–2400	450–950	900–2400	480–1450	1400–3200
Spectral resolution/nm	2–7	3–12	2.4–6.5	3.6–9.5	2.4–9.4	7.6–24.9
FOV/deg	8.5×8.5	ø 3.6	8.5×8.5	ø 3.6	4.17×4.17	4.17×4.17
Effective pixels	256×256	1	256×256	1	256×256	1
Quantization/bits	10	16	10	16	10	16
Sampling interval/nm	5	5	5	5	5	5

Direct public data on the crystal apertures used in these AOTF filters are not available. Nevertheless, from the reported instrument geometry and ancillary specifications, the optical aperture can be inferred to be on the order of 20-25 mm in diameter.

To maximize the usable tuning range on a single crystal, these projects employed a dual-transducer architecture. Because broadband operation of a tunable filter is ultimately limited by the difficulty of maintaining optimal electrical-acoustic matching between the RF driver and a single piezoelectric transducer across the entire band, the RF spectrum was partitioned into two sub-bands. Two distinct piezoelectric transducers were bonded to the same TeO_2 crystal, each impedance-matched and optimized for its respective sub-band. This configuration (See fig. 3) enables near-continuous spectral coverage while preserving diffraction efficiency and optical throughput, and it mitigates drive-power penalties and performance roll-off that typically appear when a single transducer is forced to operate over a very wide frequency range.

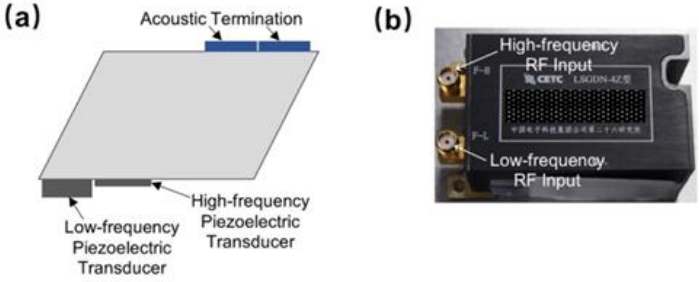

Figure 3. AOTF used on VNIS. (a) Main structure of the AOTF;
(b) The physical object of AOTF [12].

Such engineering choices further underscore China's emergence as a global leader in AOTF-based space spectrometry - advancing the field program-by-program - in contrast to the period marked by proposed funding reductions to comparable NASA efforts under the Trump administration.

Medicine

Another cutting-edge medical application of acousto-optic devices employs a different instrument class - the acousto-optic frequency shifter (AOFS).

AOFS are devices that shift the frequency of incident light by an amount equal to the applied RF drive frequency. Standard models typically provide frequency shifts above 300 MHz, available as compact low-power modules with an integrated RF driver, while custom designs can reach up to 600 MHz.

The frequency shift is generated through the anisotropic interaction of the slow shear acoustic mode in TeO_2. In this process, the undiffracted input beam and the frequency-shifted diffracted beam emerge with orthogonal polarizations. By placing an external polarizer after the AOFS, a high extinction ratio can be achieved between the shifted and unshifted beams, which is crucial for suppressing light leakage and preventing interference effects. The extinction ratio itself depends on the quality of the external polarizer rather than the AOFS.

Typical AOFS devices are highly efficient, requiring very low drive power (often below 100 mW) to produce the desired frequency shift. Designs based on the slow shear mode ensure low power consumption, though they generally exhibit a slower rise time compared to other acousto-optic interactions.

AOFS are traditionally applied in technical fields for precise, non-contact vibration measurements of both machines and large structures. However, in recent years, their use has been expanding beyond engineering, finding increasing applications in medicine as well.

In the article by Polish researchers Fiber-Based Laser Doppler Vibrometer for Middle Ear Diagnostics [4], the authors address one of the key challenges in otology: how to achieve precise measurements of ossicular vibrations when traditional laser Doppler vibrometers (LDVs) require direct line-of-sight and considerable space around the patient's head. They present a fiber-based LDV (FLDV) equipped with a handheld probe (HP), enabling use in confined anatomical regions and during endoscopic procedures. The system merges the benefits of classical vibrometers with the versatility of optical fibers. Only a probe - roughly the size of a surgical scalpel - needs to be positioned in the surgical field, while two optical fibers connect it to the central vibrometer unit, which may be located even outside the operating room.

The concept of an FLDV involves the use of a wavelength at 1550 nm, which is eye-safe radiation, commonly used in telecommunications technologies. A schema of the FLDV is illustrated in Figure 4. The coherent light source is a laser diode pigtailed to a single-mode fiber. The laser beam is then split by coupler 1 into measuring and reference beams in the ratio of 99:1. The reference beam is shifted in frequency, typically by a few tens of megahertz, using an acousto-optic (AO) Bragg shifter. The analyzed object is illuminated pointwise using a collimator (measuring beam). If the object moves, the light scattered from its surface changes frequency due to the Doppler effect. The second collimator introduces part of this scattered radiation into the fiber. The polarization controller allows for improved interference efficiency. Scattered light, which typically exhibits a power 5-6 orders of magnitude lower than the illuminating radiation, is combined with

the reference beam in coupler 2. A coupling ratio was set to 10:90. An erbium-doped fiber amplifier (EDFA) is employed for additional signal amplification before photodetection. This represents a further advantage of using 1550 nm radiation. The interference of the measurement and reference beams on the photodetector results in a frequency-modulated signal with a carrier frequency equal to the frequency of the generator powering the AO shifter.

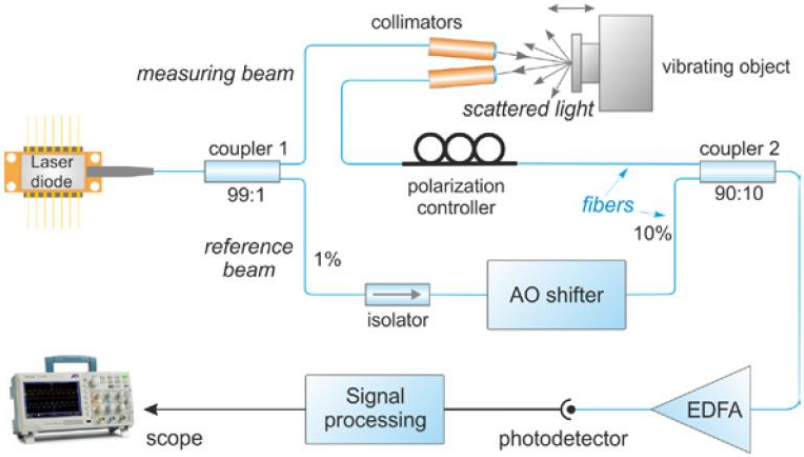

Figure 4. The concept of a fiber-based vibrometer (AO - acousto-optic, EDFA - Erbium Doped Fiber Amplifier, Fibers - standard single mode fibers) [4].

Scattered light, which typically exhibits a power 5-6 orders of magnitude lower than the illuminating radiation, is combined with the reference beam in coupler 2. A coupling ratio was set to 10:90. An erbium-doped fiber amplifier (EDFA) is employed for additional signal amplification before photodetection. This represents a further advantage of using 1550 nm radiation. The interference of the measurement and reference beams on the photodetector results in a frequency-modulated signal with a carrier frequency equal to the frequency of the generator powering the AO shifter.

The heterodyne signal from the photodetector is directed to the signal processing block, which contains the signal conditioner and demodulators (phase or frequency). Following phase or frequency demodulation, a signal with an amplitude proportional to the object's displacement or velocity is obtained, respectively.

The obtained research results served as the basis for conducting vibration tests of the middle ear ossicular chain using FLDV and were presented in detail in paper [22]. The stimulating signal consisted of four component frequencies: 0.5 kHz, 1 kHz, 2 kHz, and 4 kHz, with amplitudes determined

based on the Interacoustic AD629 audiometer (Interacoustic, Middelfart, Denmark) calibrated following ISO 389-1:1998 standards. Figure 5 shows an example of an averaged spectrum for 60 dB HL stimulation measured on a superstructure of the stapes against a noise background (the noise signal was left unfiltered).

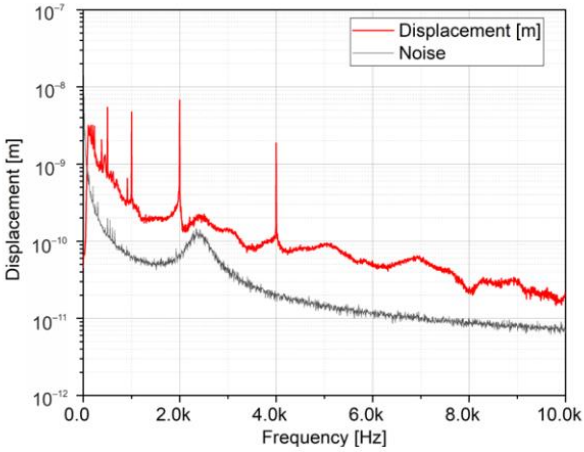

Figure 5. Averaged spectrum for 60 dB HL excitation over noise background [4].

Both the new fiber-based approach and the conventional methods employing the Polytec OFV-534 - the most widely used sensor head in ossicular displacement research [23] - rely on the same core signal-processing element, the AOFS.

Thus, acousto-optic devices are increasingly moving beyond engineering applications and becoming important tools in medical diagnostics. The use of AOFS in fiber-based laser vibrometers enables precise measurement of ossicular vibrations even in complex anatomical conditions, opening new possibilities for otology. At the same time, hyperspectral imaging based on birefringent crystals is rapidly developing, and TeO_2, thanks to its unique properties, can also demonstrate significant advantages in this field.

Quantum systems

In the previous sections, we reviewed the use of TeO_2 acousto-optic crystals in space spectrometry and medical instruments. The next important direction is their role in the rapidly growing field of quantum technologies, a development that is the result of the “second quantum revolution,” which is transforming how we process, transmit, and secure information [23].

In this context, TeO_2-based acousto-optic devices play an enabling role. Acousto-optic modulators (AOMs) and deflectors fabricated from TeO_2 are essential for quantum optics because they provide fast, precise, and low-loss control of photons - the fundamental carriers of quantum information. Their ability to shift frequency, control phase, and dynamically route single photons is critical for several applications:

- Quantum Key Distribution (QKD): QKD protocols require rapid switching between bases. AOMs in TeO_2 offer high-speed modulation with minimal added noise, ensuring high fidelity of quantum states [6].
- Quantum Memories and Repeaters: TeO_2 AOMs are used for optical switching and time-bin encoding, crucial for synchronizing entanglement distribution across long distances [24].
- Quantum Networks: NASA's SCaN roadmap emphasizes satellite-based links as a backbone of the quantum internet. "A major step forward will be the reliable and long-distance distribution of quantum entanglement, which will enable quantum repeater technology to overcome distance limitations" [23]. TeO_2 devices here can serve as frequency shifters and tunable filters, matching photonic signals across fiber and free-space channels.
- Quantum Computing with Ions or Photons: Multi-channel TeO_2 AOMs allow individual control of ion qubits by frequency and intensity modulation [25], while in photonic quantum processors, they are used for pulse picking and fast optical gating.

The paper of Canadian scientists [6] demonstrates a fast and efficient method for generating and detecting spatial modes of light, crucial for high-dimensional quantum communication and state tomography. Traditional tools like spatial light modulators (SLMs) are limited by refresh rates (~1 kHz). By introducing an acousto-optic modulator (AOM) in a double-pass configuration, the authors achieve mode switching rates up to 500 kHz, vastly outperforming SLM-only systems.

The acousto-optic modulator (AOM) plays a central role in this experiment by enabling both mode generation and mode projection. In the generation stage, the AOM deflects the laser beam according to the applied RF frequency, so that different diffraction angles illuminate separate regions of a static hologram (H1). Each of these regions encodes a distinct spatial mode, for example orbital angular momentum states, which makes it possible to switch rapidly between modes without the need to reprogram the spatial light modulator. The light then enters the AOM (Isomet 1205C-2), which is driven by RF signals with frequencies equally spaced between ν_1 = 120 MHz and ν_6 = 70 MHz, allowing precise steering of the output beam. After generation, the beam is directed to the projection stage, where it passes

through a second hologram (H2) and is analyzed with single-mode fibers and photodiodes. This arrangement enables fast quantum state tomography by projecting unknown states onto mutually unbiased bases at kilohertz rates with an average fidelity of about 97%.

The experimental setup shown in the figure 6 illustrates how the laser and AOM system are integrated. A continuous-wave 532 nm laser is first coupled through optics and directed into the AOM. The RF drive, produced by an arbitrary waveform generator and amplifiers, controls the deflection angles and thereby steers the beam across different regions of hologram H1.

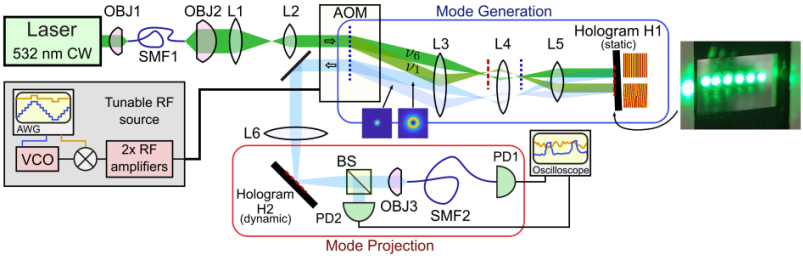

Figure 6. Scheme for rapidly switching between different spatial modes of light by using an AOM as a rapidly steerable mirror to multiplex multiple regions of a static hologram (H1). The generated modes are then analyzed using mode projection with a dynamic hologram (H2) and an SMF. Both holograms are implemented using SLMs. The blue dotted lines show the positions of object planes (near-field) of the AOM, while red dotted lines indicate the positions of the image planes (far field) of the AOM (which are also the object planes for the SLMs). Abbreviations used in the figure: acousto-optic modulator (AOM); beam sampler (BS); objective lens (OBJ); photodiode (PD); single-mode fiber (SMF); voltage-controlled oscillator (VCO) [6].

In the blue path corresponding to mode generation, multiple RF frequencies produce multiple diffraction spots on H1, each associated with a distinct spatial mode. In the red path corresponding to mode projection, the second hologram H2 selects the generated mode and projects it onto a chosen basis for detection by photodiodes PD1 and PD2. The inset photograph with six bright green spots corresponds to the simultaneous illumination of six hologram regions by different RF frequencies, which appear together in the image because the camera integrates over the rapid sub-millisecond switching of the AOM.

In summary, the experiment successfully demonstrated fast switching between six spatial modes at rates up to 500 kHz. With further optimization – such as aligning both passes of the light through the AOM closer to the transducer - switching speeds could exceed 5 MHz. The scalability of the approach can also be enhanced by employing higher-resolution SLMs or

multi-AOM configurations, enabling the generation of up to 100 modes on a single SLM. Moreover, replacing the SLM with a nanofabricated hologram would not only allow multiplexing of thousands of modes but also significantly increase the damage threshold of the device, making the system suitable for high-power and pulsed laser applications.

Chinese researchers from Tianjin University have recently presents the design and experimental demonstration of a high-performance AOM-based bi-frequency interferometer (ABI) [24]. An ABI employs acousto-optic modulators as both frequency shifters and beam splitters/combiners, enabling interference between optical fields of different frequencies. This architecture allows the device to realize either beating interference, where a modulation signal appears due to frequency difference, or beating-free interference with stable phase control. Such flexibility is highly relevant for quantum technologies, where single-photon states must be processed with high visibility and low loss.

The demonstrated ABI achieved an interference visibility of (99.5 ± 0.2)% and an optical transmission efficiency of (95 ± 1)%, significantly surpassing earlier AOM-based interferometric schemes that often exhibited visibilities below 20% [24, 26]. The authors introduced a dithering phase-locking scheme, in which the same AOM used for beam splitting also provided phase modulation. This innovation reduced the number of required optical components and improved overall system efficiency.

The indispensable role of AOMs in this setup arises from their ability to simultaneously provide high-speed frequency shifting, amplitude control, and switching. Within the ABI framework, this enables: bi-frequency coherent combination of quantum states, useful for generating large-scale entanglement; frequency tuning of quantum states, which allows spectral matching between independent quantum systems; and high-isolation optical switching, realized by gating RF signals, which is critical for protecting single-photon detectors and routing fragile quantum states [27].

Conclusions

Tellurium dioxide (TeO_2) remains one of the most versatile and efficient acousto-optic materials, combining high birefringence, strong photoelastic interaction, and low acoustic velocities. As this review has shown, TeO_2-based devices underpin a wide spectrum of modern applications: from space spectrometry, where AOTF spectrometers enable in situ mineralogical and atmospheric studies on Mars and the Moon; through medicine, where AO frequency shifters are integrated into advanced diagnostic tools such as fiber-based laser Doppler vibrometers; to quantum technologies, where TeO_2 AOMs and deflectors provide unmatched precision in frequency shifting, switching, and photon-level state manipulation.

Across these domains, one clear trend is evident: China has emerged as a global leader in many of the most promising application areas of TeO_2-based devices. The Chang'e lunar program with its VNIS and LMS spectrometers has set benchmarks for in situ planetary spectroscopy, while Chinese groups are at the forefront of developing high-performance interferometric schemes such as the AOM-based bi-frequency interferometer (ABI), achieving near-perfect interference visibility and efficiency for quantum applications. This systematic progress contrasts with the slowdown or cancellation of comparable NASA programs in recent years, further highlighting the momentum of Chinese research and engineering in acousto-optics.

Looking ahead, the unique properties of TeO_2 crystals will continue to drive innovations in hyperspectral imaging, biomedical diagnostics, secure quantum communication, and scalable quantum computing. The combination of advanced crystal growth techniques, well-established device architectures, and continuous breakthroughs in interferometric and multiplexed systems makes TeO_2 a cornerstone material of applied photonics.

References

1. Babachenko, O. I., Liubeka, I. M., Kononenko, G. A., Podolskyi, R. V., Safronova, O. A. & Agarkov K. V. (2024). Obtaining TeO_2 single crystal for acousto-optic applications: raw materials, growth process, and properties. (Review). *Fundamental and applied problems of ferrous metallurgy*, 38, 542-565. https://doi.org/10.52150/2522-9117-2024-38-542-565

2. Lim, S., Baek, S., Whitlow, J., D'Onofrio, M., Chen, T., Phiri, S., Crain, S., Brown, K. R., Kim, J., & Kim, J. (2024). Design and characterization of individual addressing optics based on multi-channel acousto-optic modulator for $171Yb^+$ qubits. arXiv:2402.13560

3. Chen, Y., Li, W., Hyyppä, J., Wang, N., Jiang, C., Meng, F., Tang, L., Puttonen, E., & Li, C. (2021). A 10-nm Spectral Resolution Hyperspectral LiDAR System Based on an Acousto-Optic Tunable Filter. *Sensors*, 19, 1620. https://doi.org/10.3390/s19071620.

4. Waz, A. T., Masalski, M., & Morawski, K. (2024). Fiber-Based Laser Doppler Vibrometer for Middle Ear Diagnostics. *Photonics*, 11, 1152. https://doi.org/10.3390/photonics11121152

5. Radpour, R., Delaney, J. K., & Kakoulli, I. (2022). Acquisition of High Spectral Resolution Diffuse Reflectance Image Cubes (350–2500 nm) from Archaeological Wall Paintings and Other Immovable Heritage Using a Field-Deployable Spatial Scanning Reflectance Spectrometry Hyperspectral System. *Sensors*, 22, 1915. https://doi.org/10.3390/s22051915.

6. Braverman, B., Skerjanc, A., Sullivan, N., & Boyd, R. W. (2020). Fast Generation and Detection of Spatial Modes of Light using an Acousto-Optic Modulator. https://doi.org/10.1364/OE.404309

7. Chang, I. C .(1981). Acousto-Optic tunable filters. *Opt. Eng.*, 20, 824–829. https://doi.org/10.1117/12.7972821

8. Harris, S. E., & Wallace, R. W. (1969). Acousto-Optic Tunable Filter. *J. Opt.*

Soc. Am., 59, 744–747. https://doi.org/10.1364/JOSA.59.000744

9. Chang, I. C. (1974). Noncollinear acoustooptic filter with large angular aperture. *Appl. Phys. Lett.* 25, 370–372. https://doi.org/10.1063/1.1655512

10. Pustovoit, V. I., & Pozhar, V. E. (1999). Acousto-optic spectrometers for Earth remote sensing. *Earth Obs. Syst.* 3750, 243–249.

11. Korablev, O., Bertaux, J.-L., Fedorova, A., Fonteyn, D., Stepanov, A., Kalinnikov, Y., Kiselev, A., Grigoriev, A., Jegoulev, V., Perrier, S., et al. (2006). SPICAM IR acousto-optic spectrometer experiment on Mars Express. *J. Geophys. Res.*, 111. https://doi.org/10.1029/2006JE002696

12. Li, J., Gui, Y., Xu, R., Zhang, Z., Liu, W., Lv, G., Wang, M., Li, C., & He, Z. (2021). Applications of AOTF Spectrometers in In Situ Lunar Measurements. *Materials*, 14, 3454. https://doi.org/10.3390/ma14133454

13. Xu, R., Li, C., Yuan, L., Lv, G., Xu, S., Li, F., Jin, J., Wang, Z., Pan, W., Wang, R., Wang, M., Xie, J., Yang, J., Wang, J., & He, Z. (2022). Lunar Mineralogical Spectrometer on Chang'E-5 Mission. *Space Science Reviews, 218*(41). https://doi.org/10.1007/s11214-022-00910-6

14. Neefs, E., Vandaele, A. C., Drummond, R., Thomas, I. R., Berkenbosch, S., Clairquin, R., Delanoye, S., Ristic, B., Maes, J., Bonnewijn, S., Pieck, G., Equeter, E., Depiesse, C., Daerden, F., Van Ransbeeck, E., Nevejans, D., Rodriguez-Gómez, J., López-Moreno, J.-J., Sanz, R., Morales, R., Candini, G. P., Pastor-Morales, M. C., Aparicio del Moral, B., Jeronimo-Zafra, J.-M., Gómez-López, J. M., Alonso-Rodrigo, G., Pérez-Grande, I., Cubas, J., Gomez-Sanjuan, A. M., Navarro-Medina, F., Thibert, T., Patel, M. R., Bellucci, G., De Vos, L., Lesschaeve, S., Van Vooren, N., Moelans, W., Aballea, L., Glorieux, S., Baeke, A., Kendall, D., De Neef, J., Soenen, A., Puech, P.-Y., Ward, J., Jamoye, J.-F., Diez, D., Vicario-Arroyo, A., & Jankowski, M. (2015). NOMAD spectrometer on the ExoMars Trace Gas Orbiter mission: Part 1—Design, manufacturing and testing of the infrared channels. *Applied Optics, 54*(28), 8494–8520. https://doi.org/10.1364/AO.54.008494

15. Bertaux, J.L., Fonteyn, D., Korablev, O., Chassefi`ere, E., Dimarellis, E., Dubois, J.P., Hauchecorne, A., Cabane, M., Rannou, P., Levasseur-Regourd, A.C., Cernogora, G., Quemerais, E., Hermans, C., Kockarts, G., Lippens, C., de Maziere, M., Moreau, D., Muller, C., Neefs, B., Simon, P.C., Forget, F., Hourdin, F., Talagrand, O., Moroz, V.I., Rodin, A., Sandel, B., & Stern, A. (2000). The study of the martian atmosphere from top to bottom with SPICAM light on mars express. P*lanet. Space Sci.*, 48, 1303–1320. https://doi.org/10.1016/S0032-0633(00)00111-2

16. Fouchet, T., Reess, J.-M., Montmessin, F., Hassen-Khodja, R., Nguyen-Tuong, N., Humeau, O., Jacquinod, S., Lapauw, L., Parisot, J., Bonafous, M., Bernardi, P., Chapron, F., Jeanneau, A., Collin, C., Zeganadin, D., Nibert, P., Abbaki, S., Montaron, C., Blanchard, C., Arslanyan, V., Achelihi, O., Colon, C., Royer, C., Hamm, V., Beuzit, M., Poulet, F., Pilorget, C., Mandon, L., Forni, O., Cousin, A., Gasnault, O., Pilleri, P., Dubois, B., Quantin, C., Beck, P., Beyssac, O., Le Mouélic, S., Johnsson, J. R., McConnochie, T. H., Maurice, S., & Wiens, R. C. (2021). The SuperCam Infrared Spectrometer for the Perseverance Rover of the Mars 2020 mission. *Icarus*. Preprint, submitted November 1, 2021. https://doi.org/10.48550/arXiv.2110.15428

17. Statement of Brimrose Corporation. Brimrose. URL:

https://www.brimrose.com/brimrose-statement

18. He, Z. P., Wang, B.,Y., Lv, G., Li, C. L., Yuan, L. Y., Xu, R., Chen, K., Wang, J. Y. (2014). Visible and near-infrared imaging spectrometer and its preliminary results from the Chang'E 3 project. *Rev. Sci. Instrum*, 85, 083104. https://doi.org/10.1063/1.4891865

19. Li, C. L., Xu, R., Lv, G., Yuan, L. Y., He, Z. P., Wang, J. Y. (2019). Detection and calibration characteristics of the visible and near-infrared imaging spectrometer in the Chang'e-4. *Rev. Sci. Instrum*., 90, 103106. https://doi.org/10.1063/1.5089737

20. Xu, R., Li, C., Yuan, L., Lv, G., Xu, S., Li, F., Jin, J., Wang, Z., Pan, W., Wang, R., et al. Lunar Mineralogical Spectrometer on Chang'E-5 Mission. *Space Sci. Rev*. (under review). https://doi.org/10.1007/s11214-022-00910-6

21. Masalski, M., Waz, A., Błauciak, P., Zatonski, T., & Morawski, K. (2021). Handheld laser-fiber vibrometry probe for assessing auditory ossicles displacement. *J. Biomed. Opt*., 26, 077001

22. Peacock, J., Dirckx, J., & Von Unge, M. (2014). Magnetically driven middle ear ossicles with laser vibrometry as a new diagnostic tool to quantify ossicular fixation. *Acta Otolaryngol.*, 134, 352–357.

23. Semenenko, H., Wright, S., Lollie, M, Flórez, J., Hoban, M., & Curchod, F. (2020). Quantum Communication 101. NASA SCaN

24. Li, W., Deng, Q., Guo, X., & Li, X. (2023). *An acousto-optic modulator based bi-frequency interferometer for quantum technology.* arXiv:2210.00406v3

25. Lim, S., Baek, S., & Whitlow, J., et al. (2024). *Design and characterization of individual addressing optics based on multi-channel acousto-optic modulator for 171Yb+ qubits.* arXiv:2402.13560v1

26. Mathevet, R., Chalopin, B., Massenot, S. (2020). Single photon beat note in an acousto-optic modulator-based interferometer. *Am. J. Phys*. 88, 313

27. Kawasaki, A. et al. (2022). Generation of highly pure single-photon state at telecommunication wavelength. *Opt. Express*, 30, 24831

І. М. Любека[1,*], начальник виробничого відділу
К. В. Агарков[1], оператор з вирощування кристалів

[1] *ТОВ «Крис-Тех», Україна*

[*] *Автор для листування: i.liubeka@crys-teh.com*

АКУСТООПТИЧНІ ПРИСТРОЇ НА ОСНОВІ КРИСТАЛІВ TeO_2: КОСМІЧНА СПЕКТРОМЕТРІЯ, МЕДИЦИНА ТА КВАНТОВІ СИСТЕМИ. (ОГЛЯД)

Анотація. Діоксид телуру (TeO_2, парателурит) залишається ключовим матеріалом у фотоніці завдяки високому акустооптичному показнику якості, сильній двопроменезаломлюваності та широкій прозорості. Пристрої на основі TeO_2 - модулятори, дефлектори та перенастроювані фільтри - широко застосовуються для керування пучком, спектрального відбіру та поляризації. У цьому огляді детально розглянуто три основні напрями, у яких такі пристрої стали критично важливими: космічна спектрометрія, медицина та квантові

технології. У космічних дослідженнях акустооптичні перенастроювані фільтри (AOTF) з TeO_2 інтегровані у провідні наукові інструменти, такі як NOMAD (ESA, ExoMars), SuperCam (NASA, Perseverance), а також спектрометри місій Китаю Chang'e. Ці системи забезпечують високороздільний спектральний аналіз поверхонь і атмосфер планет, розкриваючи інформацію про мінералогію, леткі речовини та потенційну придатність до життя. У медичній сфері акустооптичні частотозсувні пристрої (AOFS) та волоконно-оптичні лазерні доплерівські віброметри на основі TeO_2 дозволяють здійснювати точні, неінвазивні вимірювання вібрацій слухових кісточок середнього вуха. Такі системи використовуючи безпечне та гнучке телеком-діапазонне випромінювання, відкривають нові можливості в отологічній діагностиці. Використання TeO_2 підкреслює міждисциплінарний характер акустооптики, яка об'єднує фізику, інженерію та медицину. Квантові технології - це, можливо, найперспективніший напрям. Акустооптичні модулятори та дефлектори з TeO_2 є незамінними для керування світлом на рівні окремих фотонів: швидкого частотного зсуву, фазової стабілізації, маршрутизації та генерації просторових мод. Завдяки можливості інтегруватися у бі-частотні інтерферометри та багатоканальні квантові мережі, ці пристрої стають ключовими елементами квантового інтернету, квантових комунікацій та масштабованих квантових обчислень. У цілому, такі перспективні напрями вимагають не лише масштабування виробництва TeO_2-кристалів, але й постійного підвищення їхньої якості. Метою цього огляду є демонстрація конкретних прикладів застосування пристроїв на основі TeO_2 у різних галузях та підкреслення їхнього зростаючого значення для фотоніки нового покоління.

Ключові слова: діоксид телуру, акустооптичні пристрої, акустооптичний перенастроюваний фільтр, акустооптичний модулятор, акустооптичні частотозсувні пристрої, космічна спектрометрія, квантові комунікації, квантова інтерферометрія.
Посилання для цитування: Любека І. М., Агарков К. В. Акустооптичні пристрої на основі кристалів TeO_2: космічна спектрометрія, медицина та квантові системи. (Огляд). *Фундаментальні та прикладні проблеми чорної металургії.* 2025. Вип. 39. С. 309-324. https://doi.org/10.52150/2522-9117-2025-39-19

Рукопис надійшов до редакції / Received 17.07.2025
Рекомендовано до друку / Accepted 21.10.2025